ELSEVIER

Journal of Fluorine Chemistry 107 (2001) 235–240

JOURNAL OF FLUORINE CHEMISTRY

www.elsevier.com/locate/jfluchem

Fluoride crystals and high lying excited states of rare earth ions

M.F. Joubert[a,*], Y. Guyot[a], B. Jacquier[a], J.P. Chaminade[b], A. Garcia[b]

[a]*Laboratoire de Physico-Chimie des Matériaux Luminescents, U. Claude Bernard Lyon 1,UMR 5620 CNRS, 43 Bd du 11 Novembre, F-69622 Villeurbanne Cedex, France*

[b]*Institut de Chimie de la Matière Condensée de Bordeaux, UPR 9048 CNRS, 87 Avenue du Dr Albert Schweitzer, F-33608 Pessac Cedex, France*

Received 8 July 2000; received in revised form 18 September 2000; accepted 28 September 2000

Abstract

We present the advantage of fluoride crystal hosts for the study of high lying localised excited states of rare earth ions. Special attention is devoted to the study of broad band UV emissions for solid state tuneable UV lasers and to the illustration of photoionisation mechanisms involving indium ions.

Keywords: Rare earth spectroscopy; Luminescence; Photoionisation

1. Introduction

The best known optical characteristic of fluoride materials is their high transparency arising from low energy phonons on one hand and high ionicity on the other hand. These intrinsic properties extend transmission to far UV and IR, and lead to less absolute fundamental absorption with respect to other oxide or sulphide materials. Furthermore, in many chemical compositions exhibiting high solubility for rare earth ions together with crystal field effects, high doping level is achievable. Altogether, it results very efficient materials, which are used in a wide range of optical applications from phosphors to lasers.

When a rare earth ion (RE^{3+}) is embedded into a crystalline lattice, some of its well localised energy states belonging to the $4f^n$ ground electronic configuration or the $4f^{n-1}5d$ first excited configuration are located between the valence band and the conduction band of the host. UV or X-ray photoelectron spectroscopy can estimate the position of the RE^{3+} ground state relative to the top of the valence band. It appears that the location of the $4f^n$ ground state in this bandgap (E_G) is very close to the top of the valence band [1]. The advantage of fluorides is their broad bandgap, usually more than 10 eV [2]. So, the optical window where the host is transparent is wide enough to record in quite good conditions, absorption peaks attributed to RE^{3+} electronic transitions in the UV and even in the VUV spectral domain as well as emission originating from such high lying localised RE^{3+} states. As 4f electrons are protected against neighbour ion interactions by the full $5s^2$ and $5p^6$ shells, the electronic structure of $4f^n$ configurations is almost independent of the host. So, when a photon promotes an electron from the ground state to $4f^n$ excited levels, the resulting intraconfigurational transitions give rise to sharp peaks easy to assign. But for higher energy photons, an electron initially in the ground state is promoted to $4f^{n-1}5d$ levels via dipolar electric parity allowed transitions. This results in intense absorption bands widely vibronic in character due to the large radial extension of the 5d orbitals and, for the same reason, strongly dependent on the neighbouring ligands. After such excitation to $4f^{n-1}5d$ levels, fluorescence may arise either from radiative deexcitation of these $4f^{n-1}5d$ states or via nonradiative relaxation to $4f^n$ states followed by sharp $4f^n \rightarrow 4f^n$ emission lines. This depends on the energy gap between the lowest $4f^{n-1}5d$ state and the $4f^n$ level just below and on the maximum energy of phonons in the host.

A lot of interest has been recently devoted to luminescence of high excited $4f^{n-1}5d$ states of rare earth ions in crystalline hosts. This is due to the interest in broadband UV absorption or emission for various applications such as: phosphors emitting visible light upon VUV excitation for mercury-free fluorescent tubes or plasma display panels, scintillator materials, solid state tuneable UV lasers for photolithography, photochemistry, ...

In the second part of this paper, we present a brief review of rare earth doped systems in which stimulated emission of

* Corresponding author. Tel.: +33-0472-44-83-39; fax: +33-0472-43-11-30.
E-mail address: joubert@pcml.univ-lyonl.fr (M.F. Joubert).

0022-1139/01/$ – see front matter
PII: S0022-1139(00)00364-X

the $4f^{n-1}5d \rightarrow 4f^n$ UV broad band transitions was demonstrated after optical pumping into $4f^{n-1}5d$ levels. We underline the main problem which appears under high energy photon pumping, which is the solarisation effect due to photoionisation and trapping of the electron leading to colour centre formations. Then, we discuss the advantage of using upconversion-pumping processes to avoid this kind of problem and we present recent results in this field.

On the other hand, photoionisation processes are positive effects which have received a great attention recently due to their technological applications (optical memories, crystal scintillators, . . .) and also from a basic research viewpoint as the photorefractive effect. In the third part of this paper, we try to model photoionisation mechanisms. We are concerned with a reversible photoionisation process between two impurities, namely RE^{3+} (Ce^{3+}, Tb^{3+}) and In^{3+} in elpasolite fluoroindates A_2BInF_6 (A: K, Rb; B: Na, K) which appear attractive ionic host crystals for rare earths. Then, we review our recent efforts to analyse the electron donor acceptor mechanism taking advantage of the luminescent properties of the excited species involved.

2. Study of broad band UV emissions for solid-state tuneable UV lasers

In the last few years, it has been shown that the $4f^{n-1}5d \rightarrow 4f^n$ broadband interconfigurational transitions can be useful for new tuneable all-solid-state lasers. Up to now, broad band UV lasers of this type was demonstrated only in Ce^{3+} or Nd^{3+}-doped fluoride single crystals. Concerning Ce^{3+}-doped systems, due to the very simple $4f^1$ configuration (the ground $^2F_{5/2}$ manifold and only one excited $^2F_{7/2}$ manifold around 2000 cm^{-1}), emission of the 5d states which are located in the near UV is easy to observe. UV laser based on this $5d \rightarrow 4f$ transitions was first demonstrated at 325 nm with Ce:$LiYF_4$ [3] then at 286 nm with Ce:LaF_3 [4], optically pumped at 249 nm using a KrF laser. But, serious problems were induced by the formation of transitory or permanent colour centres. Such colour centre formation was essentially due to absorption of the pump and/or the laser radiation from the emitting 5d states leading to promotion of an electron into the conduction band followed by trapping by impurities or defects. For this reason, this type of solid-state laser has been discarded for many years. Then since a few years, efforts were performed by different teams to increase the efficiency of these UV lasers and spectacular results were reported with $LiCaAlF_6$:Ce [5–7], $LiSrAlF_6$:Ce [6,8] and Ce:$LiLuF_4$ [9]. Recently, slope efficiencies of more than 50% were obtained with Ce:$LiLuF_4$ pumped with either a Ce:LiSAF laser at 290 nm [10] or the frequency doubled yellow output (289 nm) of a copper vapour laser [11] and tuneability was achieved continuously from 305 to 333 nm [11]. Concerning Nd^{3+} doped systems, laser action based on $4f^25d \rightarrow 4f^3$ transitions was only demonstrated in two fluoride hosts. It was first at 172 nm by pumping a Nd:LaF_3 crystal with incoherent Kr_2* radiation at 146 nm [12]. Then laser radiations at 172 and at 260 nm had been obtained from Nd:LaF_3 and Nd:$LiYF_4$ crystals, respectively after pumping with an F_2 pulsed discharge molecular laser at 157 nm [13,14]. The maximum slope efficiency was 21%, so quite good, but saturation of the laser output was rapidly taking place due to loss mechanisms probably similar to those that occur in Ce^{3+}-doped crystals such as formation of colour centres via excited state absorption phenomena.

To avoid generation of colour centres under direct pumping in the $4f^{n-1}5d$ states of RE^{3+} ions, excitation of these states via upconversion processes (which produce populations in an excited state whose energy exceeds that of the pump photon) can be considered. Indeed, it has been shown that upconversion pumping can give rise to efficient laser emissions ($4f^n$–$4f^n$ transitions) in rare earth doped crystals (see [15] for a review). And the possibility to get a tuneable $4f^{n-1}5d \rightarrow 4f^n$ laser emission after upconversion pumping, which has never been demonstrated up to now, looks exciting. Since a few years, three research teams in France[#] have collaborated on this subject. Interesting results were obtained in Pr^{3+}-doped crystals (oxides or fluorides in which the 4f5d lowest states are located below the $^1S_0$ $4f^2$ manifold). Depending on the host material, $4f5d \rightarrow 4f^2$ broad emission bands are generally located in the near UV spectral domain (233–333 nm in Pr:$YAlO_3$, 220–280 nm in Pr:$LiYF_4$, 220–340 nm in Pr:KY_3F_{10}, . . .). Upconversion pumping of the 4f5d states was realised via two step absorption using $^1D_2$ or ^3P_J, $^1I_6$ manifolds as intermediate absorbing states and excited state absorption cross sections are of the order of 10^{-18} cm^2 [16–18]. Energy transfer from 4f5d states of Pr^{3+} to 5d states of Ce^{3+} was also observed after two step excitation into the 4f5d states [18] which suggests possibility of upconversion pumping for a UV laser based on the $Ce^{3+}5d \rightarrow 4f$ emission. In Lyon, we recently focused our attention to several Nd^{3+}-doped crystals to try to find interesting and efficient upconversion excitation into $4f^25d$ states. With Nd^{3+}, due to the presence of high energy $4f^3$ terms (a lot of terms between 30000 and 35000 cm^{-1}, $^2F(2)$ around 40000 cm^{-1} and $^2G(2)$ around 49000 cm^{-1}) and also due to higher phonon energies in oxides than in fluorides, emission from $4f^{n-1}5d$ states is not observed in oxide crystals. So, we worked only with fluoride-based crystals and a summary of our results is presented below.

The $4f^3$ energy level scheme of Nd^{3+} ions which, as mentioned previously, is almost independent of the host, and which was precisely studied in a lot of fluorides, shows three well known metastable states $^4F_{3/2}$, $^2P_{3/2}$ and $^4D_{3/2}$. Concerning the use of one of them as intermediate state for ESA upconversion pumping of $4f^25d$ levels, $^4F_{3/2}$ and $^4D_{3/2}$ can be easily pumped by convenient sources such as IR laser diode for the first one and third harmonic generation (355 nm) of Nd:YAG laser for the latter. So, we first focused on these two metastable states.

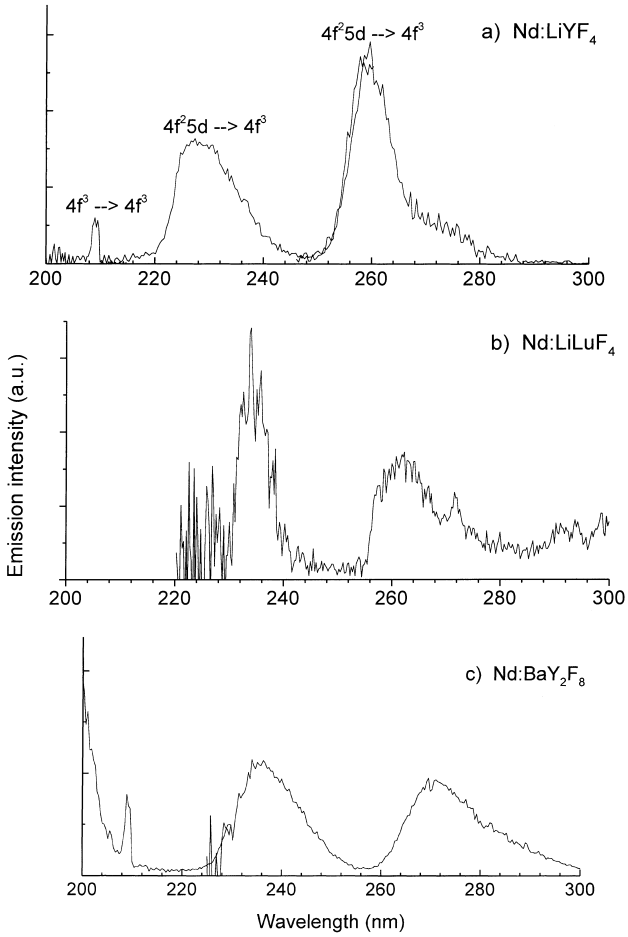

Fig. 1. Room temperature emission spectra of (a) $LiYF_4$: 1.6 at.% Nd; (b) $LiLuF_4$: 0.29 at.% Nd and (c) BaY_2F_8: 0.4 at.% Nd crystals after excitation at 355 nm.

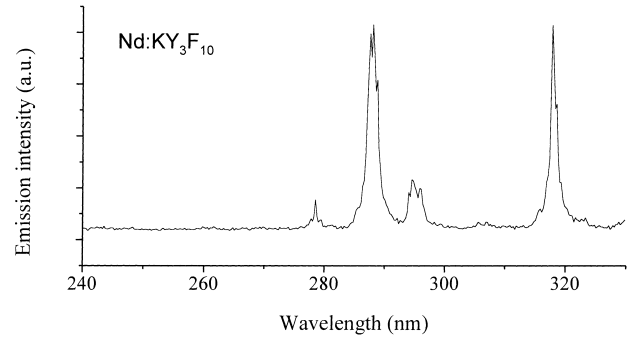

Fig. 2. Room temperature emission spectrum of KY_3F_{10}: 1.51 at.% Nd crystal after excitation at 355 nm.

The location of $4f^25d$ levels was studied in many Nd^{3+} doped fluorides and it appears that, in most of them, the successive absorption of two 355 nm photons may lead to a population in the lowest Nd^{3+} $4f^25d$ band. This is for example the case in Nd:$LiYF_4$, Nd:$LiLuF_4$ and Nd:BaY_2F_8 in which the absorption to the lowest $4f^25d$ band starts around 56000 cm^{-1} [19–21]. Fig. 1 shows UV emission spectra recorded between 200 and 300 nm in these crystals after excitation at 355 nm. It consists of two broad bands. The one at higher wavelength is attributed to the $4f^25d \rightarrow {}^2G_{7/2} + {}^2H_{11/2}$ transition and the second is attributed to the $4f^25d \rightarrow {}^2H_{9/2}$ transition. The weaker and sharp peak at 210 nm, which presents longer lifetime (about 600 ns instead of about 20 ns for the two broad bands), is attributed to the intraconfigurational ${}^2G(2)_{9/2} \rightarrow {}^4I_{11/2}$ transition. In Nd:BaY_2F_8 crystal, an increase of the signal on the lower wavelength side of the spectrum is due to another interconfigurational emission band attributed to the $4f^25d \rightarrow {}^4I_j$ transition and peaking at 190 nm [19]. As mentioned above, such Nd^{3+} broad band UV emissions cannot be obtained under 355 nm excitation in all Nd^{3+} doped fluoride crystals. Indeed, in LaF_3 or KY_3F_{10} for example, the crystal field splitting is much lower so the lowest $4f^25d$ band is located much higher, around 62500 cm^{-1} [21]. Fig. 2 illustrates the case of Nd:KY_3F_{10} for which the emission spectrum recorded under 355 nm excitation is composed of narrow lines attributed to radiative transitions from the $4f^3$ ${}^2G(2)_{9/2}$ manifold. This illustrates quite well the strong dependence of the 5d orbitals on the neighbouring ligands and, of course, the importance of the choice of the host for the Nd^{3+} activator.

In the Nd^{3+}-doped fluoride crystals showing broad band UV emissions under 355 nm pumping, transmission measurements permitted to estimate the ESA cross section in the 350–320 nm range of the ${}^4D_{3/2} \rightarrow 4f^25d$ transition. Even at the wavelength leading to the best absorption (330 nm for Nd:$LiYF_4$), the ESA cross section is estimated to be less than 10^{-20} cm^2 [20,21]. This is very low and indicates that, unfortunately, the upconversion pumping using a 355 nm laser will not be efficient enough for generating tuneable $4f^25d \rightarrow 4f^3$ UV radiations. On the other hand, $4f^3 \rightarrow 4f^25d$ transition selection rule considerations permit to suggest efficient upconversion possibilities using 355 nm photons for the first step to promote ions into ${}^4D_{3/2}$, but higher energy photons for the second step ${}^4D_{3/2} \rightarrow 4f^25d$ [22]. Moreover, excited state absorption spectra using ${}^4F_{3/2}$ as the intermediate absorbing level show two strong bands centred at 213 and 190 nm with Nd:$LiYF_4$, Nd:$LiLuF_4$ and Nd:BaY_2F_8; and the associated ESA cross section is now of about 10^{-18} cm^2 [22]. These recent results are extremely promising regarding the potentiality of Nd-doped fluoride crystals as tuneable UV upconversion lasers using two different but convenient pump beams.

Regarding this study of broad band UV emissions in rare earth-doped fluoride crystals, we need to find other fluoride hosts for RE^{3+} ions, which would be complementary or more convenient than those we already studied. Hexafluoroelpasolites would be quite interesting as they are characterised by a tight rare earth dopant site and a strong local crystal field [23,24], leading to a large Stokes shift between $4f^{n-1}5d$ band emission and absorption. This results in $4f^{n-1}5d$ band emissions that would be broader and at longer wavelength than in other complementary fluorides. Moreover, concentration quenching (migration of the energy via

radiative transfers followed by transfer to traps) would be lower and $4f^{n-1}5d$ band emission yield would be higher. With this idea, we plan to study Rb_2NaYF_6:Nd and Rb_2NaYF_6:Pr crystals which are in preparation in Bordeaux following the experimental procedure developed in the next section.

3. Study of the photoionisation mechanisms

In this part, we pay attention to a photosensitization process taking place in indium compounds doped with rare earths (namely, cerium and terbium that both are stable in several ionised states). This process was first recognised to interpret the lack of cerium luminescence in Ce^{3+}-doped indium oxide compounds where the ionised state of Ce^{3+} could not be stabilised [25]. Then it was shown that fluoride indium hosts were much more adapted to incorporate Ce^{3+}. Ternary fluoride indium compounds were found to combine both easy rare earth doping, high indium content and O_h site symmetry.

3.1. Sample preparation and crystal growth

The alkali fluorides, KF and RbF were commercial products, which were dehydrated under vacuum. The fluorides MF_3 were obtained by precipitation followed by heat treatment. Nitrates of indium, yttrium, terbium or cerium were first dissolved in distilled water and then poured into a 40% HF solution. The precipitate obtained after centrifugation was washed with water and immersed in a small amount of 40% HF which was eliminated by evaporation. In order to remove OH groups in the initial powder, a thermal treatment was accomplished at 500°C under argon in the presence of a fluorinated atmosphere created by decomposition of added NH_4HF_2 or HF gas.

Rb_2KInF_6:Ce^{3+}, Rb_2KInF_6:Tb^{3+} and Rb_2KYF_6:Tb^{3+} elpasolites with 1% of Ce^{3+} or Tb^{3+} ions have been prepared by solid state reaction from stoichiometric mixtures of compositions $2RbF + KF + (1-x)In$ (or Y) $F_3 + xCe$ (or Tb) F_3. The reactions were carried out at about 700°C in sealed gold tubes.

The Bridgman method has been selected for crystal growth. The crystal growth equipment was made of two independent furnaces separated by an insulating zone. The temperature of each furnace has been separately programmed. The powder was introduced in a platinum-10% rhodium biconical shaped crucible, which was sealed under a dry argon atmosphere and set in the crystal growth apparatus. Initially heated to $T = T_f + 50$ K in the upper furnace, the crucible was moved down to the cooler furnace at a rate of 0.5–2 mm/h with a thermal gradient of 1.5–3.0 K/mm. The temperature was then lowered to room temperature at a rate of 50 K/h.

After sawing off the upper part of the platinum crucible, crystals were removed mechanically. Transparent colourless single crystals up to cubic centimetre were obtained without visible inhomogeneities. Single crystals were oriented by X-ray diffraction, cut into slices along different crystallographic orientations with a diamond wire and polished with alumina powder in an alcoholic solution.

3.2. Photoionisation mechanisms

Polished and oriented cerium or terbium doped Rb_2KInF_6 single crystals are used for luminescent measurements at temperatures from 290 K to liquid helium. As expected, Ce^{3+} and Tb^{3+} luminescences are clearly identified as a result of $5d \rightarrow 4f$ and $4f \rightarrow 4f$ electronic transitions, respectively.

For cerium luminescence (Fig. 3), a blue-green broad band emission peaking at 480 nm is observed when excited with a 315 nm radiation. This emission is attributed to cerium ions substituting In^{3+} ions. Two other emissions with lower intensity have been detected at 320 and 425 nm for an excitation at 245 and 270 nm, respectively that are assigned to Ce^{3+} in rubidium and potassium sites, respectively [26,27].

For terbium luminescence, an O_h site of Tb^{3+} ions (probably substituting In^{3+} ions) is found and the identification and assignment of the pure magnetic-dipole transitions split out of the Tb^{3+} transitions have been achieved assuming a thermal equilibrium set of crystal field sublevels [28]. Also, a C_{2v} distortion of the octahedral site is detected at low temperature that could be due to the well-known phase transition to monoclinic structure of this material.

Under UV excitation at around 240 nm (41600 cm^{-1}) and only with a special preparation in the case of Rb_2KInF_6:Ce^{3+}, the two doped compositions exhibit characteristic fluorescence spectra composed of two broad band emissions (Fig. 4) [29]. Because of their temperature dependence of intensities and decays, they have been attributed to the presence of monovalent Indium (In^+) ions which are known to belong to the spectroscopic family of ns^2 filled

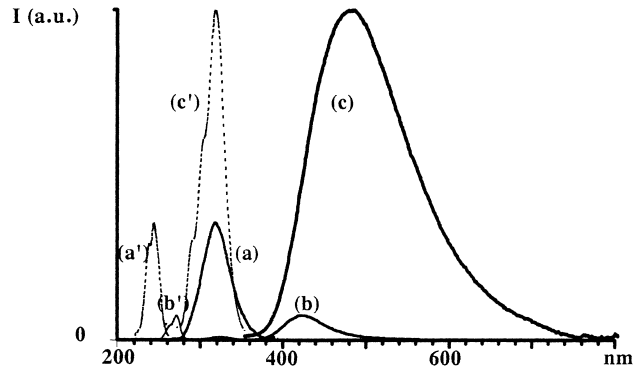

Fig. 3. Emission and excitation ultraviolet spectra (a) ($\lambda_{exc.} = 245$ nm) (a′) ($\lambda_{emi.} = 320$ nm), blue (b) ($\lambda_{exc.} = 270$ nm) (b′) ($\lambda_{emi.} = 425$ nm) and blue-green (c) ($\lambda_{exc.} = 315$ nm) (c′) ($\lambda_{emi.} = 475$ nm) luminescence of a Rb_2KInF_6:Ce^{3+} 1% single crystal at 300 K (comparable intensities, corrected from the spectral response of the photomultiplier and lamp flux).

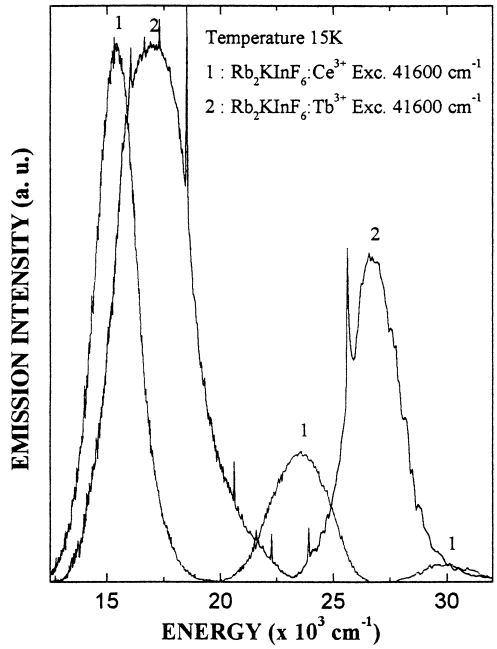

Fig. 4. Comparison among the emission spectra, at 15 K, of $Rb_2KInF_6:Ce^{3+}$ and $Rb_2KInF_6:Tb^{3+}$ elpasolites under excitation at 41600 cm^{-1}.

shell ions such as Ga^+, Tl^+, ... The peak positions of these two bands are shifted towards higher energy when substituting Ce^{3+} to Tb^{3+} as expected from the size difference of the doping ions. In a pure cubic site symmetry (such as in alkali halides) and depending upon values of the electronic parameters (electronic exchange, spin orbit coupling constant, crystal field splitting, ...), lowest In^+ excited states, so-called A (triplet $^3P_1$ excited level of the nsnp excited electronic configuration), are perturbed by the Jahn–Teller effect (JTE) giving rise to the well-known A_T and A_X emission bands. The evolution with temperature of the emission spectra and fluorescence decays follows nicely the theoretical prediction of the adiabatic potential energy surface model.

In^+ ions are unusually detected in the two doped crystals though stoechiometry is closely respected. We checked that pure Rb_2KInF_6 does not exhibit any fluorescence under the same excitation condition, which could infer the presence of monovalent indium during the growing technique. In the case of the cerium-doped fluoride elpasolite-type fluoroindate, it has been clearly established that steady-state UV excitation at 315 nm (31600 cm^{-1}) induces a gradual decrease of the intensity of the main blue-green emission together with the emergence and growing intensity of the red fluorescence at around 650 nm (15500 cm^{-1}). This is a permanent effect but completely reversible process either by steadily excited the sample at around 245 nm or the original state can be thermally regenerated after 1 h annealing at 400°C under vacuum in a sealed quartz tube. As we said before, no formation of new emitting centres have been detected under the same UV excitation in yttrium or scandium elpasolites showing that only indium and cerium are involved in the process. The photoionization mechanism has been proposed as follows [26,27]:

$$2Ce^{3+} + In^{3+} \leftrightarrow 2Ce^{4+} + In^+$$

which can be decomposed into donor and acceptor elementary processes [30]:

$2Ce^{3+} \rightarrow 2Ce^{4+} + 2e^-$ with an energy E_D and $In^{3+} + 2e^- \rightarrow In^+$ with an energy E_A. From this it is clear that the energy positions of the ground state of each ion within the gap (E_G) is of importance. They are not known yet but we can expect that the donor process promotes the electron to the conduction band because of the efficiency of the indium luminescence.

On the other hand, in the case of terbium doped indium elpasolite, the process is not so clearly observed. Indeed, following the same experimental procedure as for the cerium-doped compound, no indium luminescence is detected under UV cw lamp excitation. Low fluence UV pulsed laser excitation at 240 nm provided by a frequency double pumped dye excimer laser allows detection of In^+ luminescent ions. Furthermore, taking advantage of the blue to UV upconversion mechanism within terbium ions [28], high fluence excitation at 480 nm was proposed to achieve photoionisation of Tb^{3+} ions as for cerium ions:

$$2Tb^{3+} + In^{3+} \leftrightarrow 2Tb^{4+} + In^+$$

this process being possible because of the known stability of Tb^{4+}. This effect should be followed by an increase of In^+ ion population detected by pumping the system at 240 nm as previously. No such variation of In^+ fluorescence intensity was observed with and without blue laser excitation, even for concentrated materials up to 80%.

Assuming that no In^+ ion is present in starting materials for preparation as shown before by testing pure indium elpasolite, we cannot rule out that the oxidation–reduction process takes place during the growth of the terbium doped compound. On the other hand, the very poor efficiency of this process could be related to an energy mismatch between the donor and acceptor states together with a high stabilisation of the ground level of Tb^{3+} ions within the gap of the material. Indeed, the size of trivalent terbium ion is much closer to In^{3+} than Ce^{3+}, which should lower the energy of the ground level together with a higher E_D energy. In any case, we expect a low cross section of the effect in terbium compounds because of the lower absorption strength of the first excited states of the f–d transitions compared to cerium ions. In order to analyse more carefully all these processes, we are presently investigating CaF_2 single crystal codoped Ce^{3+} and In^{3+} on one hand and Tb^{3+} and In^{3+} on the other hand.

4. Conclusion

Different mechanisms such as broad band UV luminescence, energy transfer, photoionisation and colour centre

formation can arise from photon interaction with the RE^{3+}-doped solid in the high energy region (UV spectral domain). Upconversion pumping offers wide opportunities to use the great capabilities of interconfigurational $4f^{n-1}5d \rightarrow 4f^n$ transitions of rare earth ions in fluoride crystals in the quantum electronic. Indeed, it could allow to excite high lying $4f^{n-1}5d$ states by two or more low energetic quantums and avoid photochemical transformations in the crystal. We plan to investigate new rare earth-doped fluoride single crystals to optimise UV emission efficiency under upconversion pumping as well as to get better knowledge in photoionisation processes. It is clear that, to control all these mechanisms, it is necessary to know the energy band structure of the crystal as well as the energy positions within the forbidden bandgap of the localised energy levels of each rare earth ion involved and will also make an effort in this direction.

Acknowledgements

M.-F. Joubert is indebted to Stéphan Guy (Laboratoire de Physico-Chimie des Matériaux Luminescents, Lyon) for his participation in the study presented in Section II and to A. Cassanho (Center for Materials Science and Engineering, MIT), A.A. Tkatchuk (Laboratory of Spectroscopy of Crystals, S.I. Vavilov State Optical Institute, Saint Petersburg) and V.V. Semashko (Laboratory of Quantum Electronics and Radio-Spectroscopy, Kazan State University) for providing the Nd-doped fluoride crystals studied.

B. Jacquier and J.-P. Chaminade thank Miguel Bunuel and Bernard Moine (Laboratoire de Physico-Chimie des Matériaux Luminescents, Lyon) for their participation in the study presented in Section III.

The ''Cristaux pour sources laser accordables dans le domaine visible ou UV'' team of the Laboratoire de Physico-Chimie des Matériaux Luminescents (Université Claude Bernard Lyon 1), the ''Spectroscopie laser'' team of the Laboratoire de Traitement du Signal et Instrumentation (Université de Saint-Etienne) and the ''Matériaux et instrumentation laser'' team of the Centre Interdisciplinaire de Recherche Ions Lasers (Université de Caen).

References

[1] D. Bouttet, C. Dujardin, C. Pédrini, W. Brunat, D. Tran Minh Duc, J.Y. Gesland, in: Proceedings of the International Conference on Inorganic Scintillators and Their Applications SCINT95, Delft University Press, The Netherlands, 1996, p. 111.
[2] J.C. Krupa, M. Queffelec, J. Alloys Comp. 250 (1997) 287.
[3] D. Ehrlich, P. Moulton, R. Osgood, Opt. Lett. 4 (1979) 184.
[4] D. Ehrlich, P. Moulton, R. Osgood, Opt. Lett. 5 (1980) 339.
[5] M.A. Dubinskii, V.V. Semashko, et al., J. Mod. Opt. 40 (1993) 1.
[6] J.F. Pinto, L. Esterowitz, G.J. Quarles, Elect. Lett. 31 (1995) 2009.
[7] Z. Liu, H. Ohtake, N. Sarukura, M.A. Dubinskii, V.V. Semashko, A.K. Naumov, S.T. Korableva, R. Abdulsabirov, Jpn. J. Appl. Phys. 36 (1997) L1384.
[8] C.D. Marshall, S.A. Payne, et al., J. Opt. Soc. Am. B 11 (1994) 2054.
[9] M.A. Dubinskii, V.V. Semashko, et al., Laser Physics 4 (1994) 480.
[10] P. Rambaldi, R. Moncorgé, J.P. Wolf, C. Pédrini, J.Y. Gesland, Opt. Commun. 146 (1998) 163.
[11] A.J.S. McGonigle, S. Girard, D.W. Coutts, R. Moncorgé, Elect. Lett. 35 (1999) 1640.
[12] R.W. Waynant, P.H. Klein, Appl. Phys. Lett. 46 (1985) 14.
[13] M.A. Dubinskii, A.C. Cefalas, E. Sarantopoulou, S.M. Spyrou, C.A. Nicolaides, R. Abdulsabirov, S.T. Korableva, V.V. Semashko, J. Opt. Soc. Am. B 9 (1992) 1148.
[14] A.C. Cefalas, M.A. Dubinskii, E. Sarantopoulou, R. Abdulsabirov, S.T. Korableva, A.K. Naumov, V.V. Semashko, C.A. Nicolaides, Laser Chem. 13 (1993) 143.
[15] M.-F. Joubert, Opt. Mat. 11 (1999) 181.
[16] S. Nicolas, M. Laroche, S. Girard, R. Moncorgé, Y. Guyot, M.F. Joubert, E. Descroix, A.G. Petrosyan, J. Phys.: Condens. Matter 11 (1999) 7937.
[17] M. Laroche, A. Braud, S. Girard, J.L. Doualan, R. Moncorgé, M. Thuau, L.D. Merkle, J. Opt. Soc. Am. B 16 (12) (1999) 1.
[18] S. Nicolas, E. Descroix, Y. Guyot, M.F. Joubert, R. Abdulsabirov, S.T. Korableva, A.K. Naumov, V.V. Semashko, Opt. Mat., accepted for publication.
[19] R. Vissert, P. Dorenbos, C. van Eijk, A. Meijerink, H. den Harto, J. Phys.: Condens. Matter 5 (1993) 8437.
[20] S. Guy, Y. Guyot, A. Tkatchuk, I. Razumova, M.-F. Joubert, J. de Phys. IV 10 (2000) 109.
[21] Y. Guyot, S. Guy, J.Y. Rivoire, A. Tkatchuk, I. Razumova, C. Pédrini, M.-F. Joubert, Rencontre ILUM'99, supp of Le vide: science technique et applications, p. 13.
[22] Y. Guyot, S. Guy, M.F. Joubert, J. Alloys Compounds, accepted for publication.
[23] B.F. Aull, H.P. Jenssen, Phys. Rev. B 34 (1986) 6640.
[24] B.F. Aull, H.P. Jenssen, Phys. Rev. B 34 (1986) 6647.
[25] T. Gaewdang, Ph.D. thesis, Bordeaux, 1995.
[26] J.P. Chaminade, A. Garcia, T. Gaewdang, M. Pouchard, J. Grannec, B. Jacquier, Radiation Effects Defects Solids 135 (1995) 137.
[27] J.P. Chaminade, A. Garcia, Romanian J. Opt. 5 (1997) 15.
[28] M.A. Buñuel, L. Lozano, J.P. Chaminade, B. Moine, B. Jacquier, Opt. Mat. 13 (1999) 211.
[29] M.A. Buñuel, B. Moine, B. Jacquier, A. Garcia, J.P. Chaminade, J. Appl. Phys. 86 (1999) 5045.
[30] D.S. McClure, W.C. Wong, S.A. Basun, Radiation Effects Defects Solids 135 (1995) 27.